15

The Lund gluon model, its kinematics and decay properties

15.1 Introduction

In this chapter we consider the way in which gluons are introduced into the Lund string fragmentation model, [7], [18], [104]. They are treated as *internal excitations on the massless relativistic string* (the MRS) similar to a sudden 'hammer hit' on an ordinary classical string. Thus they will be initially well localised in space-time. But we will find that they quickly disperse their energy-momentum to the surrounding string. This property means that *the gluon excitation disappears and reappears periodically as a localised energy-momentum-carrying entity during the string cycle.*

We will start as usual with a classical mechanics scenario and study some simple modes of motion of the MRS in order to get acquainted with the notion of an internal excitation. We start with the mode which has acquired the poetical name of 'the dance of the butterfly'. It certainly does exhibit the grace and the beauty that goes with this name. After a brief snapshot description of the appearance of this mode in space coordinates we proceed to a description in space-time. This will lead us to the general equations of motion for the MRS and to an understanding of the way the string is built up in terms of moving wave fronts.

After that we consider more complex modes, although there is no reason to go into too many details. The intention is simply to provide a sufficient understanding of the basics in this kind of string motion in order to make it possible to understand the way a string which has aquired a bend will fragment.

One property which is both useful and rather easily understood is the fact that *the space-time surface spanned by the string is a minimal surface.* We will spend some time considering this notion. We will also stress the notion of *infrared stability*, which is closely related to the minimal surface properties. This means that a small disturbance, such as a small or

https://doi.org/10.1017/9781009401296.015 Published online by Cambridge University Press

collinear gluon excitation, does not change the string surface more than in a correspondingly small and local way.

After a brief description of the way fragmentation is handled (the whole process is a direct generalisation of the way a 'straight' string decays) we will turn to the consequences. We consider the correspondence in the bent string to the mean hyperbola decay, which was typical for the simple straight $q\bar{q}$-string in Chapter 9. We will find a noticeable similarity between the $(1+1)$-dimensional scenario and the multidimensional twistings and bends of the general string state.

In particular it is possible to generalise the rapidity variable for the simple straight string to a new variable which we have called λ in [48]. After we have introduced the cross section for gluon emission in Chapters 16 and 17 we will show how to calculate in an analytic form the properties of the λ-distribution and related variables. These distributions are governed by irregularities related to the so-called anomalous dimensions of QCD.

Within this pictorial scenario of gluon emission in the Lund model it is easy to understand both the increase in the multiplicity and the local properties of transverse flows. We will continue with a few remarks on *heavy quarkonia decays*. States such as the J/Ψ and Υ can, owing to their quantum numbers, decay only into three (or more) gluon final states. Such states are described in the Lund model by means of closed strings, the gluon excitations pulling out the string. Therefore there are differences between the decay of such a quarkonia state and that of a corresponding state with almost the same mass but outside the resonance (referred to as 'in the continuum'). We will explain the reason why there are more particles produced at the resonance, with its closed string state, than in the continuum with an open-ended string ending on a $q\bar{q}$-state.

15.2 The dance of the butterfly

1 Snapshots of the motion

In this section we will use some of the results from earlier investigations of string motion (cf. Chapter 6), in particular local energy-momentum conservation due to causality (cf. also Chapter 12). We consider the situation depicted in Fig. 15.1, where at the start the two endpoint particles q and $\bar{q}$ both have momentum $k_\perp$ along the same direction transverse to the connecting (straight) string (length $2l \geq 2k_\perp/\kappa$). As before we describe the ensuing motion in terms of a few snapshots in time.

A After a time δt both endpoints have moved outwards in a straight line, in the same way as for the motion described in Chapter 12 (in that case only one endpoint moved transversely). There are two

https://doi.org/10.1017/9781009401296.015 Published online by Cambridge University Press

string segments, starting out with velocities $v = \cos(\pi/4) = 1/\sqrt{2}$, as indicated in Fig. 15.1. These have energies $2\kappa\delta t$, transverse momenta $\kappa\delta t$ upwards and compensating longitudinal momenta $\pm\kappa\delta t$.

The endpoints have each lost $\kappa\delta t$ in energy and transverse momenta and the remaining straight string is also $2\delta t$ shorter. In this way we account for all the available energy-momentum just as in Chapter 12. This part of the motion will continue until all the original energy and transverse momenta of the q and $\bar{q}$ have been used up.

B After that the q and $\bar{q}$ will start to move towards each other, each gaining energy and (oppositely directed) momentum at a rate of κ. The two connecting string segments continue inwards as two fronts, each with energy $2k_\perp$ and transverse momentum $k_\perp$, and with longitudinal momenta $\pm k_\perp$ respectively.

During this phase they serve as 'transporters' of energy-momentum to the two endpoints. More precisely they pick up energy from the remaining straight string piece, thereby gaining energy at the lower end and losing it to the endpoint particles at the upper end. This part of the motion continues until the fronts meet at a time $t = l$ and it again coincides with the results of Chapter 12.

The next part of the motion is, however, both surprising and beautiful.

C After a time δt the meeting point of the fronts has, for purely geometrical reasons, moved upwards by a distance δt and each front is now $\delta t\sqrt{2}$ shorter. Therefore each front has lost energy $2\kappa\delta t$, transverse momentum $\kappa\delta t$ and longitudinal momentum $\pm\kappa\delta t$. The two endpoint particles have gained energies $\kappa\delta t$ and longitudinal momenta $\pm\kappa\delta t$ (i.e. the joint longitudinal momentum loss vanishes).

The remaining energy and transverse momentum $2\kappa\delta t$ are gathered at the meeting point of the fronts. This point has moved upwards with the velocity of light (i.e. the same velocity as the endpoints) and is evidently gaining energy-momentum at a rate 2κ! This part of the motion will continue until the two endpoints $q, \bar{q}$ and the internal excitation, called g, meet at a transverse distance $k_\perp/\kappa$ from the starting position of the system.

D After another time period δt, the q and $\bar{q}$ have passed each other and are now at a distance $2\delta t$ and moving outwards. The g continues upwards and there are two new string segments connecting the three particles. Each segment moves with velocity $v = 1/\sqrt{2}$, as indicated in Fig. 15.1, and therefore has energy $2\kappa\delta t$, transverse momentum $\kappa\delta t$ and longitudinal momentum $\pm\kappa\delta t$.

https://doi.org/10.1017/9781009401296.015 Published online by Cambridge University Press

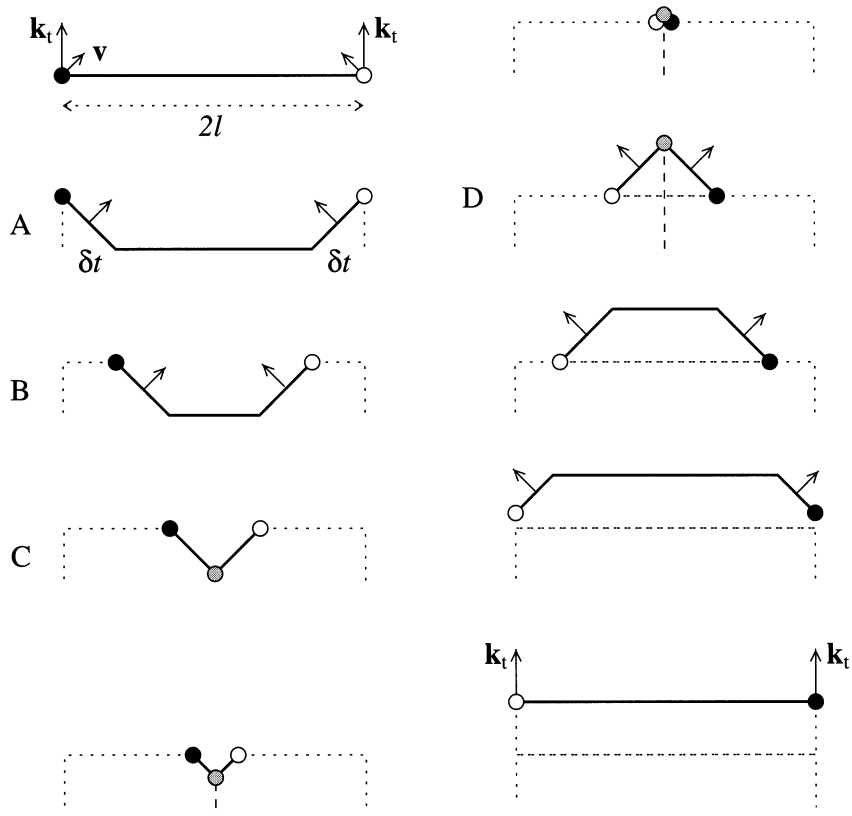

Fig. 15.1. The butterfly-dance mode of the MRS with the velocity v of the string segments and the different situations described in the text exhibited. The quark (antiquark) is denoted as an open (solid) circle and the gluon when it appears as grey. The arrows denote the directions of motion of the particles and the string segment fronts and the orbits of the quark and antiquark are shown as dotted.

> The q and $\bar{q}$ have each lost the energy $\kappa\delta t$ and the longitudinal momentum component $\kappa\delta t$. *The remaining energy and momenta in the moving string segments stem from the internal g-excitation, which has lost* $2\kappa\delta t$ *both in energy and transverse momentum* (it is useful for the reader to calculate the amount of energy-momentum in the fronts and thereby the amount which must stem from the g-excitation).

The internal excitation, the g, is evidently connected to the string in the same way as the q and the $\bar{q}$, except that the string tension acts with a force 2κ on the g. This can be understood intuitively from the fact that there are two connecting segments to the g and only one to each of the

https://doi.org/10.1017/9781009401296.015 Published online by Cambridge University Press

q and $\bar{q}$; we will see this property in more detail later. The g-excitation encountered in this way evidently has particle properties, i.e. it carries energy-momentum in a local way and *in the Lund model it is used as a model for a gluon*, just as the energy-momentum-carrying endpoints are used as models for a quark and an antiquark.

The motion described under A-C above takes a time $l + k_\perp/\kappa$ and corresponds to a quarter of the full cycle of the butterfly dance. The motion following this is depicted in Fig. 15.1 for the next quarter-cycle also. It can easily be extrapolated from what we already know. After half a cycle we are back in the starting situation except that the q and $\bar{q}$ have changed places. It takes another half period before they are back in their original positions.

We note that the total energy E is $2\kappa l + 2k_\perp$ and the total momentum P is $2k_\perp$ and is transversely directed. The total period of motion before we are back in the starting position is therefore, as usual, $2E/\kappa$ and we also note that the system has moved a distance $2\mathbf{P}/\kappa$ during this period.

The g-particle is evidently only present as a point particle during $4k_\perp/\kappa$ of the full period. During the remaining time, $4l$, it has been transformed into two inward- or outward-moving fronts on the string. This is, of course, also the way any excitation on an ordinary rubber band will perform (try it on your kitchen table, which hopefully will have little friction, with a real rubber band!).

In order to exhibit the Lorentz covariance of this picture we describe in Fig. 15.2 how the motion will appear in a different frame, in this case the cms of the system. It is again perfectly feasible to trace the motion using the same simple rules of local energy-momentum conservation as we have used repeatedly. The reader is encouraged to carry through the calculations in order to see the details.

2 *The space-time picture*

We will next provide a picture of the Lund gluon model in space-time. We use the notion of a *light ray* to describe a lightlike direction in space-time, e.g. the direction of the energy-momentum of one of the partons. We will also use *lightcone distance* to refer to the distance such a massless parton will move before it changes direction.

In Fig. 15.3 we show at the top the situation at the time of meeting of the three particles. This corresponds to a quarter-period after the start, in the description of Fig. 15.1. The subsequent motion is then considered in the cms and is therefore a space-time version of Fig. 15.2. The two endpoints move outwards along their lightcones and the string at first consists of two segments moving between the light rays of qg

https://doi.org/10.1017/9781009401296.015 Published online by Cambridge University Press

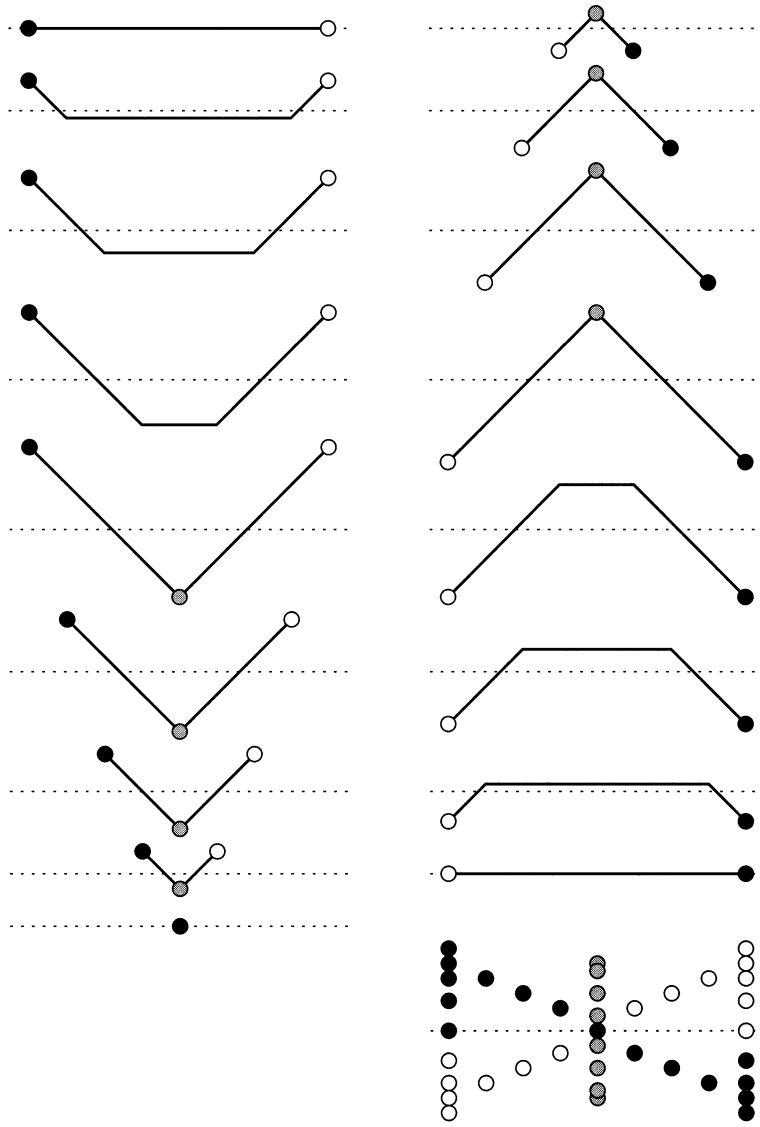

Fig. 15.2. The butterfly mode in the cms, using the same conditions and notation as in Fig. 15.1. The actual orbits of the quark (open circles), the antiquark (solid circles) and the gluon (grey circles), whenever it appears, are shown in the last combined picture.

and $g\bar{q}$, respectively. In this way the string is spanned via the g's light ray.

When the gluon has disappeared, the two segment fronts continue and there is a straight (although, in this frame, moving) string part connecting

https://doi.org/10.1017/9781009401296.015 Published online by Cambridge University Press

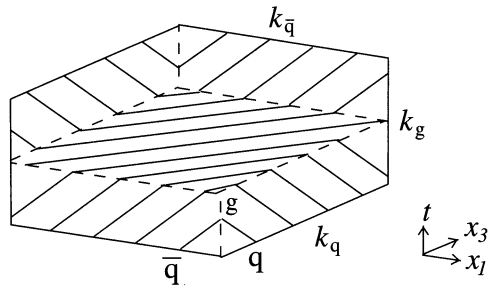

Fig. 15.3. The butterfly mode in space-time. The sets of parallel solid lines show the string at different times, the energy-momentum-carrying excitations move along the outer solid lines and the bends along the broken lines.

the fronts (see Fig. 15.2). Note that the bends between the flat part and the moving fronts of the string move along light rays parallel to the original directions of the q or $\bar{q}$.

Halfway through this (half-)period the string is totally straight. The two endpoints continue along the original direction of the g and then again two new string wave fronts are produced, which this time move inwards. The bends between the fronts and the remaining straight string again move along the lightcone directions determined by the original light rays of the q and $\bar{q}$. When the two fronts meet, the gluon reappears and the three particles approach each other, meet and separate again. During the motion the string evidently spans a surface in space-time and we will next consider some of the properties of this region.

We firstly note that all its characteristics are determined by the three lightcone distances contained in the three original excitations. In particular the right-hand, i.e. q-side, boundary line is obtained by adding in turn the energy-momenta k_q, k_g and $k_{\bar{q}}$ of the particles q, g and $\bar{q}$ (divided by κ, of course, but for the moment we will put $\kappa = 1$). Remember that the g loses twice the amount of energy-momentum per unit time to the adjoining string compared to the q and $\bar{q}$. Therefore the original lightcone distance indicated in Fig. 15.3 by g actually corresponds to half its energy-momentum, k_g. The lightcone distances that the q and $\bar{q}$ move, after using up their original energy-momentum, correspond to the true size of g's energy-momentum.

Thus the first conclusion is that the boundary line, which corresponds to the motion of the q, is given by $k_q + k_g + k_{\bar{q}}$, while the corresponding boundary line for the $\bar{q}$ is $k_{\bar{q}} + k_g + k_q$. We will soon find that there is a direct generalisation of this property to more complex string motions. In particular, everything q does is done in the opposite order by $\bar{q}$.

The corresponding conclusion for the g is that we may describe it either in terms of the motion of the right front's bend (i.e. that closer to q) or

https://doi.org/10.1017/9781009401296.015 Published online by Cambridge University Press

the left front's bend; cf. the figure. The paths are $k_g/2 + k_q + k_{\bar{q}} + k_g/2$ or $k_g/2 + k_{\bar{q}} + k_q + k_g/2$ respectively; these are the same space-time orbits as for the $\bar{q}$ and q except that they are displaced in space-time. It is again possible to generalise this result.

To that end we define a four-vector-valued function $A(\xi)$, called the *directrix*, with the following properties ($e_q, e_g, e_{\bar{q}}$ correspond to the energies of the three particles)

I If $0 < \xi \leq e_q$, then $A(\xi) = k_q(\xi/e_q)$.

II If $e_q < \xi \leq e_q + e_g$, then $A(\xi) = k_q + k_g(\xi - e_q)/e_g$.

III If $e_q + e_g < \xi \leq e_q + e_g + e_{\bar{q}}$, then $A(\xi) = k_q + k_g + k_{\bar{q}}(\xi - e_q - e_g)/e_{\bar{q}}$.

IV $A(\xi) = -A(-\xi)$.

V $A(2E + \xi) = A(\xi) + 2(k_q + k_g + k_{\bar{q}})$, with $E = e_q + e_g + e_{\bar{q}}$.

The orbit of the q, i.e. what we have referred to as the right-hand boundary line, is then $A(t)$ and the corresponding orbit for the $\bar{q}$ is $[A(t + E) + A(t - E)]/2$ (this should be checked by the reader). It is less easy to convince oneself that the orbit of the right-hand bend discussed above is given by $[A(t + e_q) + A(t - e_q)]/2$ and that of the corresponding left-hand bend is $[A(t + E - e_{\bar{q}}) + A(t - (E - e_{\bar{q}})]/2$. But it is worth doing because this is the general behaviour of any point on the string. We learned at the very beginning that the string does not conserve its length (nor does any rubber band on your kitchen table!). Therefore the points on the string cannot be characterised in terms of their space position only. But it is possible to characterise a point fully by means of the amount of energy possessed by the string to its right (i.e. towards the q-side) or equivalently to its left and we will now proceed to give a description of general string motion using this approach.

The result of this exercise also explains why the motion is periodically simple and in particular why a combined translation $2E/\kappa$ in time and an accompanying $2\mathbf{P}/\kappa$ in space always brings the string system back to the same situation.

15.3 The general description of string motion

1 The equations and their solutions

As we saw above, a point on a string will be characterised by means of the amount of energy available between the point and the q-endpoint. We call this parameter σ and we write $\mathbf{X}(\sigma, t)$ for the space position of the point and $e_q(t)$ for the q-particle energy at time t.

https://doi.org/10.1017/9781009401296.015 Published online by Cambridge University Press

A formula for σ is given by the integral along the string of the energy

$$\sigma = \int_{\mathbf{X}_q(t)}^{\mathbf{X}(\sigma,t)} \kappa dl \gamma(v_\perp) + e_q(t) \tag{15.1}$$

where $\gamma(v_\perp)$ as usual is $1/\sqrt{1-v_\perp^2}$.

The transverse velocity is denoted $\mathbf{v}_\perp$ and the string tension $\mathbf{T}$. The tension is everywhere directed along the string tangent $\partial\mathbf{X}/\partial\sigma$ and it should, when the string piece considered is at rest, have the size κ. From this it is evident that we must have

$$\frac{\partial \mathbf{X}}{\partial t} = \mathbf{v}_\perp, \quad \kappa^2 \frac{\partial \mathbf{X}}{\partial \sigma} = \mathbf{T} \tag{15.2}$$

There will be two extra conditions stemming from our choice of parametrisation, and from the fact that the string has no longitudinal degrees of freedom so that the velocity and the tension must be orthogonal. From a variation for fixed t of Eq. (15.1) we obtain

$$d\sigma = \frac{\kappa |d\mathbf{X}|}{\sqrt{1-v_\perp^2}} \tag{15.3}$$

This result contains an evident connection between the length of the tension vector $|\mathbf{T}|$ and the velocity. We have actually encountered and discussed this condition before. It can be expressed as in Chapter 6 as the result of time dilation. In this way we obtain the two conditions

$$\mathbf{T} \cdot \mathbf{v}_\perp = 0, \quad \frac{\mathbf{T}^2}{\kappa^2} + \mathbf{v}_\perp^2 = 1 \tag{15.4}$$

Next we note that the momentum carried by a small energy 'grain' $d\sigma$ is $d\mathbf{p} = d\sigma \mathbf{v}_\perp$ (remember that $d\mathbf{p}/de = \mathbf{v}$ for an on-shell particle). Therefore the change in momentum with time for this energy grain is given by

$$\frac{d(d\mathbf{p})}{dt} = \mathbf{T}(\sigma + d\sigma) - \mathbf{T}(\sigma) \quad \Rightarrow \quad d\sigma \frac{\partial^2 \mathbf{X}}{\partial t^2} = d\sigma \kappa^2 \frac{\partial^2 \mathbf{X}}{\partial \sigma^2} \tag{15.5}$$

Thus we obtain (after division by $d\sigma$) the usual wave equation for the motion of the points on a string (i.e. in the limit when the energy-momentum grains referred to above become infinitesimal). We therefore conclude that the general solution must be

$$\mathbf{X}(\sigma, t) = \tfrac{1}{2}[\mathbf{B}(t + \sigma/\kappa) + \mathbf{C}(t - \sigma/\kappa)] \tag{15.6}$$

where $\mathbf{B}$ and $\mathbf{C}$ are two arbitrary vector-valued functions. This solution corresponds to two moving fronts and we will now consider suitable boundary conditions to determine them. These conditions are simple in this case because we note that *for an open string with endpoints the tension of the string must vanish at the endpoints.* Therefore for $\sigma = 0$ and $\sigma = E$,

https://doi.org/10.1017/9781009401296.015 Published online by Cambridge University Press

E being the total string system energy, we must have

$$\kappa^2 \frac{\partial \mathbf{X}}{\partial \sigma} = 0 \tag{15.7}$$

Expressed in terms of $\mathbf{B}, \mathbf{C}$ this means

$$\dot{\mathbf{B}}(t) = \dot{\mathbf{C}}(t), \quad \dot{\mathbf{B}}(t + E/\kappa) = \dot{\mathbf{C}}(t - E/\kappa) \tag{15.8}$$

where the dots indicate derivatives. The two equations can be readily integrated and we may write

$$\mathbf{B} = \mathbf{C}, \quad \mathbf{B}(t + 2E/\kappa) = \mathbf{B}(t) + 2\mathbf{P}/\kappa \tag{15.9}$$

Therefore the general solution can be expressed in terms of a single function $\mathbf{B}$:

$$\mathbf{X}(\sigma, t) = \tfrac{1}{2}[\mathbf{B}(t + \sigma/\kappa) + \mathbf{B}(t - \sigma/\kappa)] \tag{15.10}$$

with the requirement that $\mathbf{B}$ should be periodic, with a constant translation $2\mathbf{P}/\kappa$ over the period $2E/\kappa$. In particular we note that the q-endpoint moves along the function $\mathbf{X}(0, t) = \mathbf{B}(t)$ and the $\bar{q}$ along $\mathbf{X}(E, t) = [\mathbf{B}(t + E/\kappa) + \mathbf{B}(t - E/\kappa)]/2$.

The conditions in Eq. (15.4) mean that

$$\dot{\mathbf{B}}^2 = 1 \tag{15.11}$$

i.e. the endpoints always move with the velocity of light.

We have in this way obtained a complete description of any string with endpoints. In particular we find that the results for the simple $qg\bar{q}$-state described in the earlier section is true for all points on the string. The directrix function A defined there evidently coincides with the four-vector $(\xi, \mathbf{B}(\xi))$. (The result is easily generalisable to a string with many gluons and this is a useful exercise. We will later discuss an example with two gluons.) The condition IV on the directrix A is, however, peculiar to a string which passes through a single space-time point, i.e. the point where the three particles start out.

We will end this section with a few considerations on the energy-momentum content of a string region. We note the relation used above for the energy grains, $d\mathbf{p} = d\sigma \mathbf{v}_\perp$. From this we may by introducing our solution calculate the total momentum flowing across a spacelike surface in the region ABCD, depicted in space-time in Fig. 15.4.

The region is limited by the two sets of curves $t - \sigma$ and $t + \sigma$ equal to constants ($\kappa = 1$ again for simplicity). The parameter values are for A (t, σ_1), for B (t, σ_2) and for the pair CD the 'earlier' and 'later' crossing points.

Then we obtain by integrating out the energy-momentum content in

https://doi.org/10.1017/9781009401296.015 Published online by Cambridge University Press

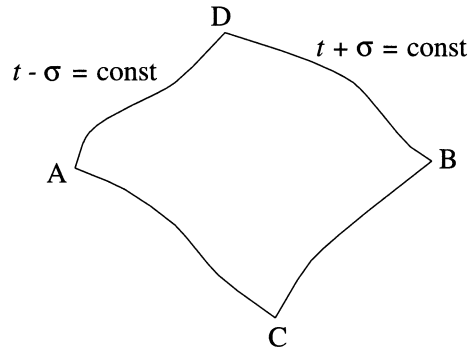

Fig. 15.4. The points A and B are at a spacelike distance (we choose equal times) and there is a region spanned by them and the points C (earlier) and D (later), which is the causal dependence region.

between A and B at the fixed time t,

$$\begin{aligned}\mathbf{P}_{AB} &= \int_A^B d\sigma \frac{\partial \mathbf{X}}{\partial t} \\ &= \tfrac{1}{2}[\mathbf{X}(t+\sigma_2) + \mathbf{X}(t-\sigma_1) - \mathbf{X}(t-\sigma_2) - \mathbf{X}(t+\sigma_1)] \\ &= \mathbf{X}_D - \mathbf{X}_C \end{aligned} \tag{15.12}$$

Thus the difference vector between two points on the string surface is directly given by the *energy-momentum that flows inside the causal dependence region.* This result was freely used in the $(1+1)$-dimensional model, where the lightcone directions coincided with the parameter curves $t \pm \sigma$ (a useful exercise is to find the directrix for the description of a straight $q\bar{q}$-string). Equation (15.12) means that this result is also true for a general string surface if we use the causal dependence region.

It is in the same way possible to calculate the energy-momentum that will flow across a timelike curve between the points C, D (note that these points have the same value of σ):

$$\int_C^D d t \mathbf{T} = \mathbf{X}_B - \mathbf{X}_A \tag{15.13}$$

This is the result first pointed out by Artru, [25], cf. Chapter 9: the momentum transfer between a group of particles moving to the left with respect to a particular breakup vertex and one moving to the right is given by the variable Γ. This variable also corresponds directly to the proper time, in this case between C and D.

https://doi.org/10.1017/9781009401296.015 Published online by Cambridge University Press

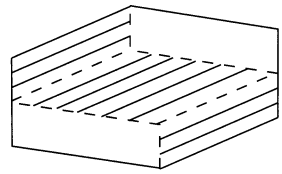

Fig. 15.5. The solid lines show how the q-side grains move, thereby translating the original energy-momentum k_q of the q leftwards across the space-time surface.

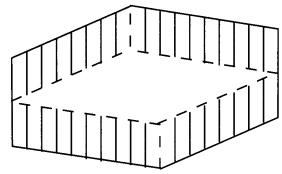

Fig. 15.6. The two sets of g-grains moving apart, thereby translating half of the original energy-momentum k_g in each direction across the space-time surface.

2 *The space-time surface of a $qg\bar{q}$-state*

We now return to the butterfly-state motion to consider the space-time surface in the light of what we learned from the general behaviour of the MRS in the last subsection. The two wave fronts described by the directrix can be thought of as a (continuous) stream of energy grains moving to the left (from the q-side) and to the right (from the $\bar{q}$-side). They move throughout with the velocity of light and can be thought of as having been emitted by the excitation particles.

The conditions in Eq. (15.7) means that the grains coming in towards the left bounce out towards the right and vice versa. Note, however, that the grains often stay at the endpoint (and the g-excitation) positions for some time. We show in Figs. 15.5, 15.6 and 15.7 the way the energy-momentum vectors 'march' across the surface, thereby spannning it.

If we follow the q-side boundary line the first part can be thought of as corresponding to emission of the k_q-grains and the next part as corresponding to absorption of (half) the k_g-grains (i.e. those sent out by the g in that direction). The part after that corresponds to re-emission of these k_g-grains and is followed by absorption of the $k_{\bar{q}}$-grains by the q.

Thus we find that the reason why the string does not keep its size is that grains may be gathered up at certain space-time positions during the cycle. These positions correspond to the excitation particles either at the

https://doi.org/10.1017/9781009401296.015 Published online by Cambridge University Press

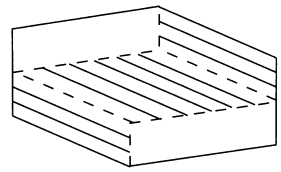

Fig. 15.7. The $\bar{q}$-side grains moving across the space-time surface thereby translating the original energy-momentum $k_{\bar{q}}$ of the $\bar{q}$.

endpoints or in the centre and they have the property to absorb or emit grains at a constant rate in space-time.

The reason that the g interacts at twice the rate of the q or the $\bar{q}$ is that in this case there are grains coming from or going towards both sides. A bend corresponds to the situation when the grains come in and go out again at the same rate.

In the same way we could describe the emergence of the straight string piece connecting the two fronts as a combination of the k_q-grains coming from the right and the $k_{\bar{q}}$-grains coming from the left, while the right (left) wave front region corresponds to the combination of half the k_g-grains with the k_q-grains ($k_{\bar{q}}$-grains).

Each region therefore corresponds to a lightcone diamond spanned by two lightcone directions, each with a length corresponding to one of the characteristic original particle energy-momenta (half for the g, however, each time).

From the results of this discussion it is easy to calculate the area of the surface for the half-period discussed. We find that $k_q k_{\bar{q}} + k_g k_q + k_g k_{\bar{q}} = (k_q + k_g + k_{\bar{q}})^2/2 = M^2/2$. This is again in accordance with our earlier result that the space-time surface area for the full period is given by the squared system mass.

At this point we would like to make a few historical remarks. At the basis of all advanced dynamics situations there can be formulated an *action principle*. Thus, according to Hamilton's principle, the motion of a system from time t_1 to t_2 is such that the line integral of the Lagrangian L,

$$I = \int_{t_1}^{t_2} dt L(x(t), \dot{x}(t)) \tag{15.14}$$

has an extremum along the path $x(t)$. Here L is expressed in terms of (possibly many) coordinates x and velocities $\dot{x}$.

This statement is closely related to the behaviour of geodesics on surfaces defined by a differential geometry and a metric. Thus a free

https://doi.org/10.1017/9781009401296.015 Published online by Cambridge University Press

relativistic point particle (mass m) will move in such a way that the (invariant) length along the path is minimal and one can choose $Ldt = -m\sqrt{(dt)^2 - (d\mathbf{x})^2} = -mdt\sqrt{1-\mathbf{v}^2}$ as the Lagrangian. The inclusion of electromagnetic fields introduces a geometry in phase space and modifies the particle motion to a new geodesic.

String dynamics can be formulated in a similar way, [62], by requiring that *a surface area should be minimal.* This can be expressed in very general forms (and in the reviews on the subject, [62], you will find very learned discussions). For the situation at hand we may formulate this surface area as a two-dimensional integral with integration element

$$d\Sigma = -\kappa dl dt\sqrt{1-\mathbf{v}_\perp^2} = -\kappa dt d\sigma \left|\frac{\partial \mathbf{X}}{\partial \sigma}\right| \sqrt{1-\left(\frac{\partial \mathbf{X}}{\partial t}\right)^2}$$
$$= -\kappa dt d\sigma \sqrt{\left(\frac{\partial X}{\partial \sigma}\right)^2 \left(\frac{\partial X}{\partial t}\right)^2 - \left(\frac{\partial X}{\partial \sigma}\frac{\partial X}{\partial t}\right)^2} \qquad (15.15)$$

In the last line we have extended $\mathbf{X}$ into a four-vector $X = (t, \mathbf{X})$.

Use of Euler's variational calculus on such a two-dimensional integral leads to the wave equation considered in Eq. (15.5). *The main point is, however, that the string surface always is a minimal surface.* That is the reason why its behaviour is directly describable by means of the boundary curve, i.e. the directrix. Every young person who ever twisted a wire into some closed shape and dipped it into soapy water has seen the beauty of the shimmering thin surface emerging and probably also noted that this minimal surface is directly related to the bends and the twists on the wire. These features correspond in the MRS to the elementary excitations on the string. This illustrates why we can describe the string surface in terms of only the endpoint $q\bar{q}$- and the internal g-excitation paths.

15.4 Multigluon states and some complications

1 On the color-flow connections

We will not study the most general multigluon scenario that is possible within the Lund model but will be content to consider a state with two gluons having a general appearance similar to the earlier one-gluon case (Fig. 15.8).

We immediately encounter the problem that there are two ways of drawing the Lund string between the excitations in this case. These ways are shown in Fig. 15.8. The two cases correspond to different *color-flow directions* around the gluon corners. Classically they are mutually exclusive but it is a complex question whether quantum mechanics will allow interference between the two color-flow states.

https://doi.org/10.1017/9781009401296.015 Published online by Cambridge University Press

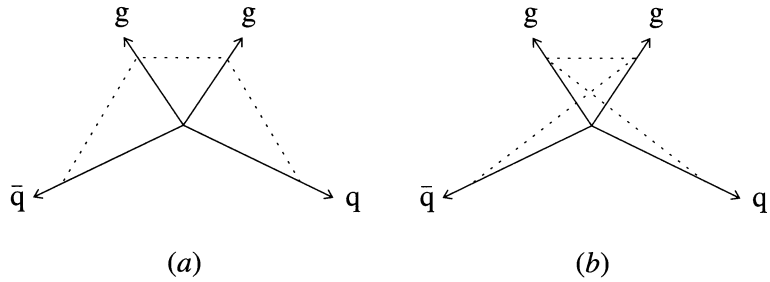

Fig. 15.8. The initial situation for a symmetrical two-gluon state with the momentum vectors of the four partons indicated. The broken and dotted lines show the string for the two possible color flows in the situation.

We will come back to the problem in Chapter 17 when we discuss multigluon bremsstrahlung emission. We note that *the question is basically whether it is sufficient to know the charges in order to obtain the fields.* This is always the case for abelian fields like those of electromagnetism. Besides very small quantum corrections due to photon-photon scattering it is always possible to describe the emerging electromagnetic fields as a superposition of the fields due to the separate charges.

One basic assumption in the Lund model is that the color electric fields do have a meaning *per se*, because all the final-state particles stem from the breakup of these fields. In a totally perturbative QCD scenario only the charges, i.e. the q, $\overline{q}$ and the g's, appear in the final state and one is, in general, summing over all their connecting color indices. Then the color-flow connection needed for the Lund model string fragmentation is not obvious. It turns out that both of the color-flow configurations described above will occur at the matrix element level as distinct contributions (cf. [71]). At the cross section level (i.e. after squaring the matrix elements) there will be interference between the color-flow configurations, however.

The interference terms are in general smaller by a factor of $1/N_c^2$ (with N_c the number of colors) compared with the terms corresponding to definite color-flow directions. Therefore one may hope that they should not be very noticeable for the observables in an actual experiment. From the point of principle they are, however, of great interest. There are some possible cases for which these corrections can be studied, [103], although there is at present no convincing experimental proof of their existence. The problem is that there are $n!$ possible color flows obtainable in connection with the general n-gluon state. Although, as we will see in the following chapters, the coherence properties

https://doi.org/10.1017/9781009401296.015 Published online by Cambridge University Press

of gluon radiation will strongly suppress most of these configurations there are nevertheless too many possible color-flow configurations left to pinpoint the differences simply from the hadrons observed in a final state.

The question, raised in this subsection, whether the field configurations in QCD are part of the state description is generally described in quantum field theory as *the problem of possible super-selection quantum numbers.* From the way the theory is formulated, in terms of the QCD Lagrangian, cf. e.g. [52], there are no clues as to whether such quantum numbers exist. Only the charges occur, in the perturbative treatments of QCD. Super-selection quantum numbers are therefore not observable unless one sums all the perturbative contributions.

2 *A two-gluon state*

Leaving aside this question we proceed to study one of the color-flows in the two-gluon state shown in Fig. 15.8. This state is the most 'natural' one in the sense that the string does not contain sharp bends. It is also the one with the largest probability of occurring owing to the above-mentioned coherence properties of gluon emission.

In Fig. 15.9 we show the space-time behaviour of this string state. It is easily understood as soon as we provide the directrix, which, this time, corresponds to the ordered curve between $k_q, k_{g1}, k_{g2}, k_{\overline{q}}$. It is obviously possible to expand the definition of the directrix in subsection 2 of section 15.2 to any number of color-connected gluons along the same lines.

We note again, in particular, how the grains transport the vectors of the elementary excitations diagonally across the surface. The initial region between the two gluons is spanned by $k_{g1}/2$ and $k_{g2}/2$ with the grains of the first coming from the left and those of the second from the right. This piece of surface appears four times during this half-cycle of the string motion, first between g_1 and g_2, next between the q and one bend, then between another bend and the $\overline{q}$ and finally in the rebuilding of the two gluon excitations.

It is also of interest to compare the situation for a single gluon in Fig. 15.3 with the one described by Fig. 15.9: note that on the surface of the butterfly-dance mode the single gluon 'ridge' along the lightcone has split up into a diamond between the two gluons. Evidently if the two gluons are close together then this diamond will approach the original single gluon ridge. In this case the two bends on the wave fronts denoted b_1 and b_2 in the figure will merge and re-form a single gluon.

This means that *the interpretation of the surface in the Lund model is infrared stable*, i.e. whether two collinear gluons are described as a single entity or as two distinct parts the surface will look the same. This property

https://doi.org/10.1017/9781009401296.015 Published online by Cambridge University Press

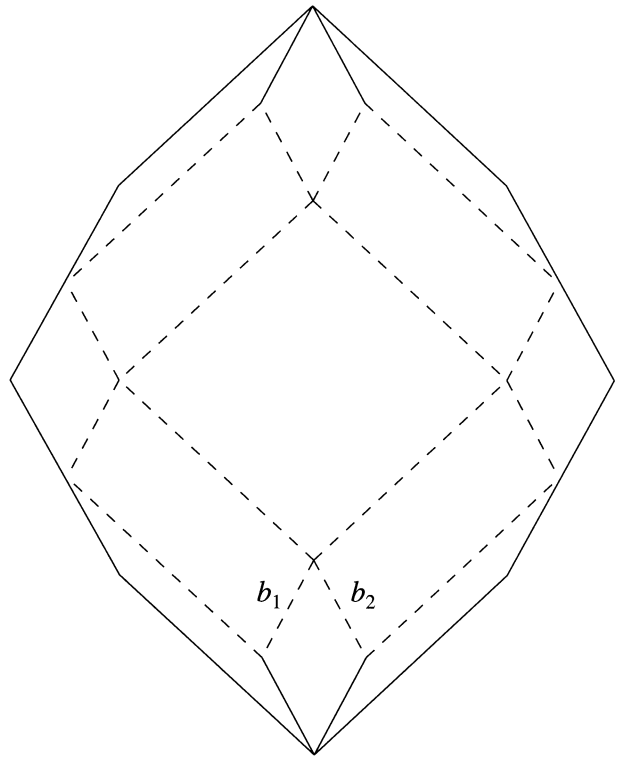

Fig. 15.9. The space-time surface spanned by a symmetrical two-gluon state.

is of the utmost importance for the success of the Lund model. The same thing is the case if one, or both, of the gluons is collinear with the q and/or the $\bar{q}$. Again some parts of the surface will become thinner until they finally coincide with the lightcone motion of the q and/or the $\bar{q}$.

If the gluon is soft and central, i.e. it contains little energy, then it will quickly become two wave fronts. In this case the wave fronts are very tiny disturbances on a basically straight string. This is again an expression of the infrared stability of the Lund string fragmentation. A soft gluon does not influence the fragmentation process; the final state will look very much as if the gluon never had been there!

In making the comparison between the two figures it is interesting that the appearance of more gluons in a certain sense 'smooths off' the string surface. Evidently a general string surface can be described in terms of lots of soft and collinear gluons crawling along 'eating' and 'spitting out' the energy grains to which we have repeatedly referred.

https://doi.org/10.1017/9781009401296.015 Published online by Cambridge University Press

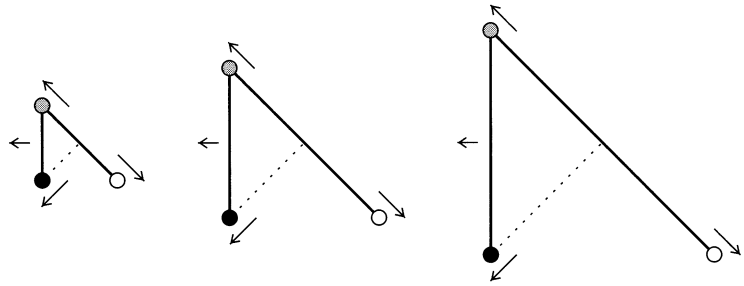

Fig. 15.10. The butterfly-dance mode after a boost such that the qg-segment of the string is at rest. The quark is shown as an open circle, the antiquark as a solid circle, the gluon grey and the directions of motion are marked with arrows.

15.5 The breakup of a gluonic Lund string

1 The possible problems

The general rules for the breakup should be the same as for the simple (1+1)-dimensional $q\bar{q}$-state we have discussed extensively before (Chapters 7–10). There are, however, complications when the string surface is no longer completely flat and we will now discuss some of them. In order to orient ourselves towards the problem we will start with the butterfly-dance mode again. This time we perform a boost transversely to the segment qg with a velocity $v = 1/\sqrt{2}$ (cf. the situation discussed in connection with Fig. 15.1).

In Fig. 15.10 we show the appearance of the $qg\bar{q}$-state after this boost. The q-particle is now moving outwards along a straight string at rest and the g is going in the other direction. At the q-end there is no reason to expect any difference from the $(1 + 1)$-dimensional model. The other segment between the g and $\bar{q}$ is of course moving away in a different direction. In the figure we show by a dotted line the path of the $\bar{q}$ in this frame. It is useful to carry through the calculations necessary to prove that the motion indicated in Fig. 15.10 really describes the situation!

We therefore assume that this part of the string segment will break up in its own rest frame, as before, and the same evidently goes for the region around the $\bar{q}$ (although that rest system is different). The difficulty occurs only in traversing the gluon corner from the straight string segment on the one side to the segment on the other (note that the segments are in general moving apart in different directions!).

There have been different suggestions in different models of how to handle a gluon corner in fragmentation. It is possible, for instance, to

https://doi.org/10.1017/9781009401296.015 Published online by Cambridge University Press

assume that the gluon is split up into a $q\bar{q}$-pair according to one or another rule. Then one would be able to handle the breakup by considering the two new strings obtained. *In the Lund model we will keep to a connected-string situation*, however.

Evidently, some difficulties may arise owing to the fact that the gluon in the Lund model is not always a pointlike particle: according to our findings, it dissolves into two wave fronts moving apart with a straight segment in between the two bends 'left over' from the g. *It turns out that there will be problems with respect to the time sequences of the breakups.* The main problem is whether it is possible to produce a scheme that has the same fragmentation results if we start the process along the straight segment on one side of the gluon corner if we start it on the other side and fragment in the opposite direction. *This turns out to be impossible* if we allow the string states to move independently in space-time. It is only for the simple $(1 + 1)$-dimensional model that the breakup of a string always produces two dynamical systems that are identical apart from their size.

To see the difficulty assume that we break the string around one of the wave front bends. Suppose we produce a $q_1\bar{q}_1$-pair in the string segment ending on the $q \equiv q_0$. Then we obtain a straight segment starting on q_0 and ending on $\bar{q}_1$ which behaves like an independent string state (and may be fragmented further in the usual Lund way). Besides the momentum transfer at the breakup this part will also continue to move as before, i.e. its space-time surface is (part of) the original string surface. The 'leftover' state with q_1 at the end and the wave front bend approaching also forms an independent string system *but this system will no longer move in space-time as before when it was connected to* q_0.

The new state will trace out a different space-time surface, which is not part of the original one. It is rather easy to convince oneself that if we trace it backwards in time then the g-excitation (from which the wave front bend stems) will be different (or even non-existent!). Therefore we obtain by this breakup two systems and one of them is not dynamically equivalent to a part of the original system.

If we instead consider a string breakup on the other side of the wave front bend, producing a $q_2\bar{q}_2$-pair, then neither the system composed of $\bar{q}_2$, the wave front bend and the straight segment to q_0 nor the remaining system ending on q_2 will behave in a simple way. They will trace out in space-time string surfaces without any simple resemblance to the original one; see for example [104]. What is even worse is that the behaviour of the subsystems depends upon the order in which we produce the $q_1\bar{q}_1$- or the $q_2\bar{q}_2$-breakups. The two production points are always at a spacelike distance (this is of course always the case for the production vertices along a Lund string!). We are, however, used to being able to introduce e.g. a proper time ordering with respect to the starting vertex. But even this

https://doi.org/10.1017/9781009401296.015 Published online by Cambridge University Press

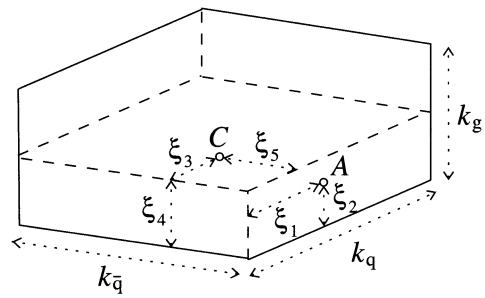

Fig. 15.11. The coordinates of some points on the string surface of the butterfly-dance mode.

proper time ordering may be different due to the fact that the produced string systems will move differently according to whether we break the string first at the $q_1\bar{q}_1$-vertex or at the $q_2\bar{q}_2$-vertex.

The conclusion of Sjöstrand's paper [104] is that *it is necessary to implement the string breakup as a process on the original string surface.* This means that we consider the string surface to be given as a 'frozen' geometrical object. Under these circumstances it is perfectly feasible to implement the symmetrical Lund model fragmentation process.

2 *The gluon fragmentation model of Sjöstrand*

We will make the following basic assumption.

- A string piece, if it fulfils the mass-shell condition, can be projected onto a hadronic state with the same probability irrespective of whether it contains at the semi-classical level internal excitations, bends etc.

Sjöstrand [104] has produced one version of a possible gluon fragmentation scheme based upon this assumption. It is incorporated into the Monte Carlo program JETSET, [105]. One of his findings in [104] is that there are only small differences between various possible schemes from the point of view of observables.

In order to describe his scheme we note that each point on the string surface can be given a 'proper time' with respect to the starting point of the original particles. In order to understand this we consider again the surface of the butterfly-dance mode (see Fig. 15.11).

The regions between the q and the g, and between the g and the $\bar{q}$, are of the same kind as we met in the $(1+1)$-dimensional model, i.e they are

https://doi.org/10.1017/9781009401296.015 Published online by Cambridge University Press

simply two lightcone regions. Consider an arbitrary point in the figure such as A and note that it can be described by means of two coordinates:

$$A = \xi_1 k_q + \xi_2 k_g \tag{15.16}$$

Therefore the squared proper time is given by $\Gamma_A = A^2 = 2\xi_1\xi_2 k_q k_g = \xi_1\xi_2(k_q + k_g)^2 = \xi_1\xi_2 M_{q,g}^2$. Its relation to an area can be inferred from the figure (we have again used dimensions such that $\kappa = 1$). The same goes for all parts of the qg and $g\bar{q}$ regions.

A more complex point is C, also indicated in the figure. It can be described as follows:

$$C = \xi_3 k_q + \xi_4 k_g + \xi_5 k_{\bar{q}} \tag{15.17}$$

where $\xi_4 = 1/2$. As for A we may identify $\Gamma_C = C^2$ and express it, this time, in terms of three coordinates ξ_j and the squared masses between the original partons. This is again an area and it is useful to construct it on the figure! There is no difficulty in convincing oneself that this procedure can be extended to any point on the surface.

It is also possible to define steps similar to the production steps in the $(1 + 1)$-dimensional model. If we imagine ourselves at the point A and would like to pick up a particular energy-momentum from the string by a step to, e.g. the point B, then if B is in the same segment as A there is again no difference from the $(1 + 1)$-dimensional case.

If B and A are in different string regions (for $B \equiv C$ we have such a case in the figure; C is on the flat string region between the two outward-moving fronts) then it is again possible to define a difference vector P_{AC} between A and C in terms of the original parton energy-momenta:

$$P_{AC} = \rho_1 k_q + \rho_2 k_g + \rho_3 k_{\bar{q}} \tag{15.18}$$

(Note that ρ_2 is determined by the starting position A and that there is a relation between ρ_1, ξ_3 and A's position, $\xi_1 = \rho_1 + \xi_3$, and one further condition, $\rho_3 = \xi_5$).

The requirement that P_{AC} should be on the mass shell then provides a condition among the coordinates ρ_j. The mass square can again be described in terms of certain areas on the surface. The main point is, however, that if we know the position of A, the size of Γ_C and the squared mass P_{AC}^2 then the position of C is also determined if it is on the string surface. (Convince yourself of that!)

The way JETSET implements the fragmentation is then step by step:

J1 With a knowledge of the original flavor (or antiflavor) a new $q\bar{q}$-pair is chosen with the probabilities described before.

J2 A meson with mass m is produced and a value of the fragmentation variable z is chosen from the symmetric fragmentation function.

https://doi.org/10.1017/9781009401296.015 Published online by Cambridge University Press

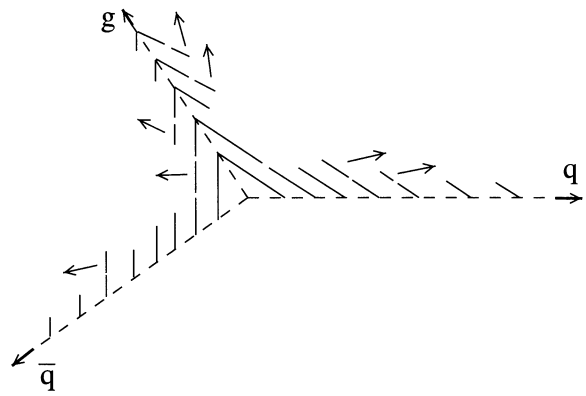

Fig. 15.12. The space-time development of a $qg\bar{q}$-state; the original directions of the partons are shown as broken lines, the string positions at different times are shown as solid lines and the momentum vectors of the emerging yoyo-hadrons are shown by the thinner arrows.

J3 The next $\Gamma_C = \Gamma_f$ is calculated from the earlier one, $\Gamma_A = \Gamma_i$, by $\Gamma_f = (1 - z)(\Gamma_i + m^2/z)$. This relation is exact in any of the 'simple' regions defined by two lightcone directions.

J4 The new breakup point is chosen as the point which has the value Γ_f and the step vector $P_{AC}^2 = m^2$. This is a unique prescription and determines the point C.

We have left out the transverse momentum generation, which is done in the same way as before, i.e. with a gaussian distribution. There are some complications about the directions that should count as transverse to the string direction in the relevant region, cf. [104]). The final mass, m, is then the transverse mass.

Some further technical problems are discussed in Sjöstrand's work, [104], but there is no need to delve into them here. We will instead turn to the experimentally observable consequences of the Lund gluon model.

15.6 The final-state particles in the breakup of a $qg\bar{q}$-state

1 General properties and the string effect

In Fig. 15.12 we illustrate the appearance of the final-state breakup in space-time for a one-gluon state. The three original excitations are moving out along the directions shown in the figure. The string is spanned via the g from q to $\bar{q}$ and a set of small final-state yoyo strings is depicted

https://doi.org/10.1017/9781009401296.015 Published online by Cambridge University Press

(for simplicity, at the moment of their emergence as independent entities) together with their space sizes and their momentum vectors.

The most noticeable thing is that most of the final-state yoyo particles move out along the three original parton directions with varying energies. The reason for this is that a moving string is Lorentz-contracted, as we have seen before. Therefore the size of one of the yoyo string pieces that moves quickly along e.g. the q-direction may appear very much smaller than one of the yoyo pieces produced at the centre. Nevertheless in its own rest system it is, of course, the same size. There will then be many more yoyo-hadrons from the seemingly small string pieces close to the trajectories of the three partons.

Quantitatively we may make the following estimates. Suppose that we consider a Lorentz frame in which the gluon goes out at an angle $\pi/2$ with respect to the q-direction. Then the longitudinal size l (i.e. the size along the q-direction) of a hadron with mass m and energy E is proportional to m/E. Such a string piece will contain an amount of gluon momentum $k_g \propto l$, i.e. $\propto 1/\cosh y$, with the rapidity y along the q-direction being calculated in this frame. Therefore we conclude that a gluonic disturbance is in general only noticeable within a small rapidity region (of order $\delta y \sim 1$) around the gluon direction (remember that angle and rapidity are connected). It will fall off as $\exp(-|y - y_g|)$ for larger rapidity differences.

There are some corrections to this, stemming from (almost) collinear gluon emission along the original gluon direction. Such emissions will tend to broaden the angular region affected around a hard parton but most of the parton energy still remains within a tiny angle even after a gluonic cascade and fragmentation; see the discussion in the following chapters.

Thus there will be three jets of particles basically along the three original directions (although there are some interesting differences between the jet directions and the original directions, to which we return).

From this picture we also conclude that the slower particles at the centre in general emerge earlier in time than the faster ones. This effect has been noted earlier and discussed in Chapter 7 in connection with the notion of the formation time.

The next experimentally observable result is that *there will be a few particles produced in the angular sectors between the q and the g and between the g and the* $\bar{q}$ *but there are none produced between the q and the* $\bar{q}$ *because there is no string spanned over this sector.* This is the nowadays well-known *string effect*, which was predicted (see [18]) before it was observed by the JADE group at PETRA.

There are several problems in disentangling this effect in an experiment, however. There are firstly the transverse momentum effects from the gaussian zero-point fluctuations. This means that the particles, which in the mean will emerge along two hyperbolas in momentum space, as

https://doi.org/10.1017/9781009401296.015 Published online by Cambridge University Press

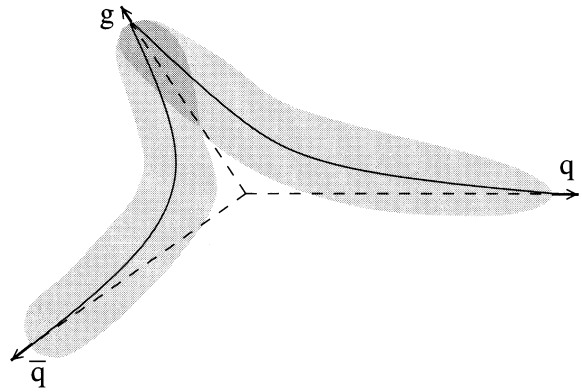

Fig. 15.13. The momentum-space picture of the final-state particles, which in the mean emerge along two hyperbolas. Due to transverse momentum fluctuations during the fragmentation the particles are diffused over the shaded regions.

shown in Fig. 15.13, are in reality diffused over the shaded areas. The typical distance of the hyperbola from the origin is of the order of 300 MeV/c, which is also the size of the transverse momentum fluctuations.

The second problem is to know which of the three jets is the gluon jet. In general the gluon jets contain less energy than the q or $\overline{q}$ jets do, but there are large variations according to the QCD emission probabilities. Nowadays this problem has diminished owing to the very large statistics produced in the LEP experiments. In these experiments it is even possible to tag one or both of the q and $\overline{q}$ jets by observing semi-leptonic heavy quark decays.

We may conclude that the string effect which was already quite noticeable in the JADE data nowadays provides strong confirmation of the existence of color-flow asymmetries in connection with gluon emission. There is, within perturbative QCD [27] also, such an effect, which is related to the coherence properties of gluon bremsstrahlung (cf. Chapters 16, 17).

It is interesting to note that if one only considers particles which have a large transverse momentum out of the production plane (the $qg\overline{q}$-state evidently defines a single plane in momentum space) then the string effect is even larger. The same applies if one considers only heavy particles, such as kaons and baryons. The reason, within the string scenario, is that the production of large (transverse) masses will use up larger pieces of the string and therefore such particles will feel more of a push from the string motion.

https://doi.org/10.1017/9781009401296.015 Published online by Cambridge University Press

2 The jet-axes problem

A general problem in e^+e^- annihilation experiments is to determine the 'true' jet-axes' directions. In this case, as compared with e.g. hadronic interactions or inelastic lepto-production, there is no obvious initial direction along which the main dynamics proceeds.

The initial annihilation current of the e^+e^--pair is in the cms directed in the plane transverse to the momentum direction of the pair, if we neglect the rest masses. This was discussed for the current matrix elements in Chapter 4. The same also goes for the current of the $q\bar{q}$-pair produced in the annihilation, with respect to their momentum directions.

Therefore there is a correlation between the initial e^+e^--direction and the $q\bar{q}$-direction, corresponding to the current overlap $|\mathbf{j}_e \cdot \mathbf{j}_q|^2 \propto (1 + \cos^2\theta)$, θ being the angle between the two directions. This is a rather soft correlation, varying only between 1 and 2.

In order to analyse the final state in an event it is therefore necessary to define some directions by means of the observed particles. Several such methods are currently in use for doing jet analysis but we will not go into many details. We would like to point out, however, that the description of the events in terms of directions defined from the events themselves almost necessarily leads to some bias.

One rather obvious possibility is to consider a tensor $I_{\alpha\beta}$ constructed from the final-state momentum vectors $\mathbf{p}_j = \sum_\alpha p_{j\alpha}\mathbf{e}_\alpha$ of the N observed particles in an event:

$$I_{\alpha\beta} = \sum_{j=1}^{N} (\mathbf{p}_j^2 \delta_{\alpha\beta} - p_{j\alpha} p_{j\beta}) \tag{15.19}$$

This tensor plays a role similar to the inertia tensor in the theory of solid bodies. Taken as a matrix it is possible to diagonalise it and to construct the eigenvalues λ_α as well as the (unit) eigenvectors $\mathbf{e}_\alpha$, $\alpha = 1, 2, 3$. From its construction we conclude that there will be a smallest eigenvalue, conventionally λ_3, and one defines the corresponding eigenvector $\mathbf{e}_3$ as the *sphericity axis* and the *sphericity* S as

$$S = \frac{3\lambda_3}{\sum \lambda_j} = \min_{\mathbf{e}} \left[\frac{3 \sum_{j=1}^{N} (\mathbf{e} \times \mathbf{p}_j)^2}{2 \sum_{j=1}^{N} \mathbf{p}_j^2} \right] \tag{15.20}$$

where the minimum corresponds to $\mathbf{e} = \mathbf{e}_3$. In this way one finds the *axis along which the sum of the (squared) transverse momenta is minimal.*

There is another way, already mentioned in Chapter 13, to find the *direction along which the sum of the longitudinal momenta is maximal, the*

https://doi.org/10.1017/9781009401296.015 Published online by Cambridge University Press

thrust axis $\mathbf{n}_T$ *such that the thrust* T *is maximal*:

$$T = \max_{\mathbf{n}} \left[\frac{2 \sum_{j=1}^{N} \Theta(\boldsymbol{n} \cdot \mathbf{p}_j) \boldsymbol{n} \cdot \mathbf{p}_j}{\sum_{j=1}^{N} |\mathbf{p}_j|} \right] \tag{15.21}$$

For events in which the observable momentum is conserved (meaning that no particle has evaded the detectors) we can change the thrust definition to

$$T = \max_{\mathbf{n}} \left[\frac{\sum_{j=1}^{N} |\mathbf{p}_j \cdot \boldsymbol{n}|}{\sum_{j=1}^{N} |\mathbf{p}_j|} \right] \tag{15.22}$$

There are no perfect detectors so the first definition is often the safer one.

It is evident that from an analytical point of view the sphericity measure is more regular. But at the same time it will give a quadratic weight to the momenta. Therefore a single particle with a large momentum will in general provide a larger contribution than a group of particles which together have this momentum.

This is particularly inconvenient if we consider an event before or after the decay of some of the particles. The thrust definition is less sensitive to these features. However, although thrust is not easy to work with analytically, it is very simple in general to generate a computer routine to find out where the thrust axis is for the observed particles in a given event. A general feature is that the thrust axis connects the two groups of particles which together have the largest (and oppositely directed) momenta. Therefore thrust directly serves as a 'handle' on the way the event looks.

Both the sphericity and the thrust variables provide a means to assess quantitatively the amount of gluon emission. For a large-energy single $q\bar{q}$-event the thrust $T \simeq 1$ and the sphericity $S \simeq 0$. They will deviate noticeably from these values for events containing one or more hard gluons because in that case a large amount of energy is moving transversely.

The string effect in the Lund model fragmentation actually produces some (minor) distortions in the particle distributions due to the way thrust and sphericity are defined. Suppose that there is a gluon emitted at a finite angle with respect to either the q- or the $\bar{q}$-direction and suppose that the mass of the two partons is not small. From this configuration we expect that some particles will be produced in the angular region between the q ($\bar{q}$) and the g.

The thrust and sphericity axes will both be tilted towards the most energetic of the q or $\bar{q}$ and the g but the particles in between will also influence the determination of the axes. In particular any jet-finding algorithm [2] would tend to create jets such that there is a slightly smaller angle between the observed directions of the qg- and $g\bar{q}$-jets than between

https://doi.org/10.1017/9781009401296.015 Published online by Cambridge University Press

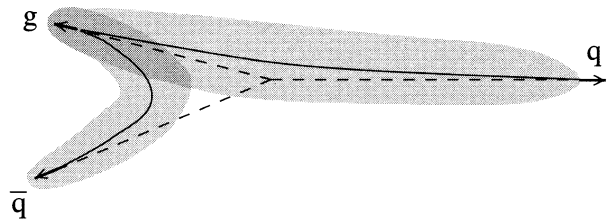

Fig. 15.14. A collinear configuration of a $qg\bar{q}$-state, and the ensuing final-state hadrons, described in momentum space.

the original parton directions, in order to accommodate the extra particles in between. The field of jet-searching algorithms is, however, still under intense development and we refer to the discussions in e.g. [2] for those readers with a technical interest in them.

3 *Infrared stability*

We have already referred to this notion. In the next chapter we will show that the cross sections for gluon emission are divergent for soft and collinear emissions. Therefore the number of gluons is not a well-defined notion but *the effect of the gluon emission is observable.* It is an essential point that if soft or collinear gluons are emitted in a bremsstrahlung process, it is their combined activity that will play a role for the fragmentation. We have already seen that the surface of the MRS is infrared stable, in the way the concept is employed in the Lund model. A soft or collinear gluon only has small and, in general, local effects.

In Fig. 15.14 we exhibit the result in momentum space for the fragmentation of a $qg\bar{q}$-state in the case where the gluon is close in angle to the $\bar{q}$. Again, the shaded area is the one inside which the final-state particles emerge. It is then noticeable that, as the mass of the $g\bar{q}$-pair diminishes towards the mass of the final-state hadrons, no hadrons are produced in between the two partons. Instead final-state particles may occur having a larger energy than any of the partons!

If we instead consider the emission of a 'soft' gluon in the centre of the event, i.e. a gluonic disturbance containing small cms energy then there are only very small effects even in the neighborhood of the gluon rapidity. In Fig. 15.15 we show again the shaded area in momentum space where the final-state particles emerge for such a soft gluon emission. The gluon is only noticeable as a small localised transverse momentum 'bump' in the distribution.

https://doi.org/10.1017/9781009401296.015 Published online by Cambridge University Press

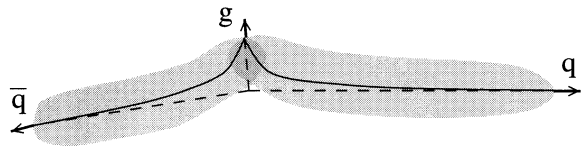

Fig. 15.15. A soft gluon emission and the ensuing final-state particles in momentum space.

As a general rule of thumb, the effect of a gluon excitation is hardly noticeable when the transverse momentum of the gluon or the gq- or $g\bar{q}$-pair's mass is smaller than 2 GeV. Actually there is a moving interface between the fragmentation and the gluon emission processes according to the Lund model. One can stop the emission of gluons basically anywhere between a cutoff at $k_\perp = 7$ GeV down to a few hundred MeV and still obtain the same distribution of final-state hadrons. One needs different fragmentation parameters, however, and we will present an interesting systematics for this phenomenon in Chapter 17.

4 *The decay of heavy quarkonia*

One of the true revolutions in high-energy physics occurred when the very long-lived resonance state, the J/Ψ, was found in October 1975. It was amazing to disentangle a state which is so massive. The J/Ψ-mass is around 3.1 GeV, i.e. about four times the ρ- and ω- masses and three times the proton and neutron masses. A more important fact was that the J/Ψ is so long lived. This meant that there must be new physics involved.

After the first few months of frantic discussions and investigations the high-energy physics world settled for the fact that there was a c-flavor quark and that the J/Ψ was a bound state, of vector character, of a $c\bar{c}$-pair. The other vector mesons, the ρ, ω and ϕ, are all built from the light quarks and all decay rather quickly; it is only necessary to produce one or two new light $q\bar{q}$-pair(s) to make them decay into a mixture of light pseudoscalar meson states.

We note that flavor is a conserved quantity in QCD-initiated reactions. For the J/Ψ (and also in connection with the later-discovered Υ, a bound state of a $b\bar{b}$-pair with mass around 9.5 GeV) the corresponding mesons, the D-states and the B-states, contain the c ($\bar{c}$) and b ($\bar{b}$) together with a light $\bar{q}$ (q). It turns out, however, that even the lightest $D\bar{D}$ ($B\bar{B}$) has too large a rest mass to allow the decay $J/\Psi \to D\bar{D}$ ($\Upsilon \to B\bar{B}$). It is then necessary either that one of the c (b) or $\bar{c}$ ($\bar{b}$) decays semi-leptonically (which we will not treat in this book; owing to the small

https://doi.org/10.1017/9781009401296.015 Published online by Cambridge University Press

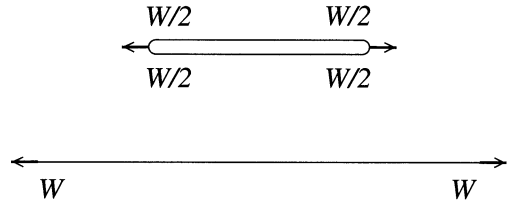

Fig. 15.16. A state in which two gluons separate, spanning two string regions each carrying a mass $s/4 = (W/2)^2$, compared with a single string spanned by a $q\bar{q}$-state of mass $s = W^2$.

coupling constants these are rather suppressed reactions) or that there is an interaction channel allowing for the annihilation of the heavy flavor and antiflavor into multigluon states.

This latter alternative requires the c and $\bar{c}$ (b and $\bar{b}$) to meet, i.e. the decay is governed by the wave function at the origin of the relative coordinates, $|\psi(0)|^2$, which serves as a form factor suppressing the decay. The possible decay channels are governed by the internal quantum numbers of the J/Ψ or the Υ. The simplest such state is a three-gluon state (but multigluon states would also be allowed).

In this case *a closed string will emerge spanned by the three gluon corners*. We have not treated this situation in the general description of string motion above, mainly because we do not need the details in a general description.

It is rather easy to imagine how the closed string is stretched and the only feature of interest for this discussion is that *it has no endpoints*. We have seen before that the existence of a string endpoint means necessarily that there is also a fragmentation region governed by the flavor at the endpoint. In practice this means a lower yield of final-state particles within 1–2 units in rapidity. For a closed string (which is the same all over) these suppressions are not available and this is particularly noticeable for baryon-antibaryon production. The gluon is flavorless. There is also the fact, to be further discussed in the next section, that the appearance of gluons increases the phase space for particle production.

As a minimum size for the increase in phase space we may imagine that one of the three gluons is very soft, so that we obtain a situation in which two gluons move out in opposite directions, as in Fig. 15.16. In the figure we also show a state with the same mass $s = W^2$, but containing only a $q\bar{q}$-pair. We note that if the total rapidity for the $q\bar{q}$-state is $(\Delta y)_q = \log(s/s_q)$, then the total rapidity within which we can produce particles will be $(\Delta y)_g = 2\log(s/4s_g)$ in the gg-state.

https://doi.org/10.1017/9781009401296.015 Published online by Cambridge University Press

The reason is that each gluon will have two adjoining string pieces and that the mass in each one must be $W/2$. If there are three hard gluons on the string the corresponding rapidity range will be even larger but it turns out that one of the gluons is in general rather soft in the process under consideration so that the approximation is well justified.

Therefore there will be a larger multiplicity for all hadrons in the case of a closed three-gluon string, although this of course depends upon the two scales s_q and s_g which govern the fragmentation. If we set $s_q = s_g = 2$ GeV^2 we obtain for Υ

$$(\Delta y)_q \simeq 3.8, (\Delta y)_g \simeq 4.8 \tag{15.23}$$

This implies that there should be around 1.3 times as many mesons on the Υ-resonance with the three-gluon decay as in the continuum surrounding it (which seems to be a reasonable approximation). *But there will be a noticeable enhancement of baryons as compared with an open string.*

According to the simple baryon-antibaryon production model discussed in Chapter 13 there is a region of around 1.5 units in rapidity, close to the endpoints, which is lost for baryon-antibaryon production. For the gluon string there is no 'flavor direction' and consequently this suppression is not available. Therefore the enhancement of baryons should in this case be very noticeable for a gg-state with the same mass as a $q\bar{q}$-state in the continuum. From the numbers above we would expect that the ratio of the number of baryons would be

$$\frac{(B\bar{B})_\Upsilon}{(B\bar{B})_{cont}} \simeq \frac{4.8}{3.8 - 1.5} = 2.1 \tag{15.24}$$

The estimates presented above are not far off the experimental results from ARGUS, although we have certainly used a very simple model!

15.7 A measure of multigluon activity, the generalised phase-space rapidity

Based upon the ideas presented in [48] we will in this section introduce a useful new variable, the total generalised rapidity λ. We will be content to consider a single hard gluon emission and extend the definition of λ to multigluon situations in section 17.4.

We have already seen that the appearance of gluonic excitations in a string state produces certain regions, close to a hard gluon emission region, where more particles will emerge. Therefore for such events there will no longer be an essentially constant rapidity plateau, which was characteristic for the simple $(1 + 1)$-dimensional $q\bar{q}$-model. (This result is independent of the axes chosen to define the rapidity variable).

https://doi.org/10.1017/9781009401296.015 Published online by Cambridge University Press

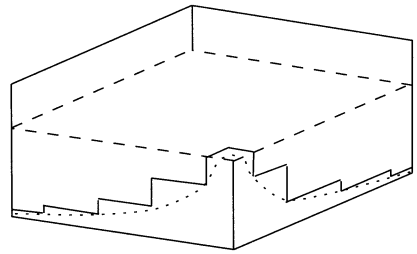

Fig. 15.17. The particles are produced along hyperbolas corresponding to fixed values of the squared proper time Γ.

It is useful to introduce some variable which follows the production region, as does the ordinary rapidity for a straight $q\bar{q}$-string. We would like such a variable to have the following properties.

- The measure λ should be well defined for each event.
- The mean value of λ should be proportional to the corresponding mean value of the multiplicity of the events.
- The distribution in multiplicity for events with a given value of λ should be almost Poissonian (although slightly narrower, as we found for the Lund model properties in Chapter 11).

We can rather easily obtain such a variable if we generalise the mean hyperbola decay picture we used in Chapter 9. There we found that the breakup vertices of the string are on the average distributed along a curve with a constant value of Γ, the squared proper time. In energy-momentum-space language the squared proper time corresponds to the squared momentum transfer between the particles produced to the left and to the right of the production vertex. From this dual relationship (cf. Figs. 9.4 and 9.5) the hyperbola decay corresponds to ladder diagram chains for which the momentum transfers are all the same.

If we consider a typical breakup, such as the one shown in Fig. 15.12, in space-time we obtain a picture like that in Fig. 15.17. We again notice the two hyperbolas in the regions between the q and the g and between the g and the $\bar{q}$ together with a few particles produced near the gluon corner.

In order to describe the situation we introduce the following notation. The total energy-momentum of the event is P_{tot} with $s = P_{tot}^2$ and the three energy-momenta of the partons are k_j, where

$$\sum_{j=1}^{3} k_j = P_{tot}, \quad s_{ij} = 2k_i k_j = (k_i + k_j)^2, \quad s = s_{12} + s_{23} + s_{13} \quad (15.25)$$

https://doi.org/10.1017/9781009401296.015 Published online by Cambridge University Press

(indices 1 and 3 represent the q and $\bar{q}$, respectively, and index 2 represents the g).

Thus we obtain a generalisation of the total rapidity range from the case where the event is of the $q\bar{q}$-type to the case where it is of the $qg\bar{q}$-type:

$$\begin{aligned} \Delta y &= 2\log(\sqrt{s}/W_q) = \log(s/s_q) \\ (\Delta y)_{gen} \equiv \lambda &= \log(s_{12}/W_g W_q) + \log(s_{23}/W_g W_q) \\ &= \Delta y + \log(s_{12}s_{23}/ss_g) \end{aligned} \tag{15.26}$$

The two terms in the definition of λ are the lengths of the two hyperbolas in the qg- and the $g\bar{q}$-sectors.

We now assume that there are regions close to the q- and $\bar{q}$- ends, respectively, that correspond to fragmentation regions, in which there is a lower density of particles. Thus we 'lose' $\log W_q = (1/2)\log s_q$ in each q- and $\bar{q}$-region. Similarly we assume that on both sides of the gluon corner there is a corresponding loss governed by $\log W_g = (1/2)\log s_g$.

We may then conclude that the rapidity region has increased owing to the emission of the gluon, and that the quantity

$$\log(s_{12}s_{23}/ss_g) \equiv \log(k_\perp^2/s_g) \tag{15.27}$$

is a measure of the increase. We will next show that the quantity $k_\perp$ occurring in Eq. (15.27) in fact corresponds to the transverse momentum of the gluon.

To see this we consider the event again in a frame where the q and $\bar{q}$ separate in opposite directions with energies e_1 and e_3, respectively. The g will move away transversely with energy e_2. Then we obtain by direct calculation that

$$\begin{aligned} s_{12} &= (e_1+e_2)^2 - e_1^2 - e_2^2 = 2e_1e_2 \\ s_{23} &= (e_2+e_3)^2 - e_2^2 - e_3^2 = 2e_2e_3 \\ s_{13} &= (e_1+e_3)^2 - (e_1-e_3)^2 = 4e_1e_3 \\ k_\perp^2 &= \frac{s_{12}s_{23}}{s} = \frac{e_2^2}{1+(e_2/2)(1/e_1+1/e_3)} \simeq e_2^2 \end{aligned} \tag{15.28}$$

the approximation being valid unless the g's energy is of the same order as the energies of the q and $\bar{q}$. Another way to obtain the result is to note that there is a direction in the cms (approximating the directions of the q and $\bar{q}$) along which $k_\perp^2$, as defined above, is identical to the gluon's transverse momentum. We will show this in Chapter 17 after we have introduced a few more kinematical notions.

The result for the phase-space extension is clear. What happens is that the single hyperbola for the flat string is exchanged for two hyperbolas, the connecting point being 'pulled out' by the gluon corner. The tip formed in this way corresponds to an extension of phase space (not only for emission

https://doi.org/10.1017/9781009401296.015 Published online by Cambridge University Press

of final-state hadrons but also for further gluon emission, cf. Chapter 17), whose size is determined by the transverse momentum of the gluon.

The size of the extension is calculated in terms of a scale s_g characteristic of the particle production around the gluon corner. In the same way the original hyperbola is measured by means of a scale s_q characteristic for production at the q- and $\bar{q}$- endpoints of the string. In the section on Υ-decay we used the estimates $s_g = s_q = 2\ \mathrm{GeV}^2$.

In section 17.4 we will consider the necessary steps for a generalisation of the λ-measure to multigluon situations. We note, however, that the present definition is only useful when the squared masses between the partons exceed the scales s_q and/or s_g and we will therefore in section 18.7 extend the definition to an infrared-stable λ-measure.

At the same time we will be able to introduce a 'local' value of the λ-measure. Up to now λ as it is defined evidently corresponds to the total available region for particle production (and, as we will later also find, for gluon emission in perturbative QCD). Therefore it is similar to Δy, the total available rapidity region for the decay of a straight $q\bar{q}$-string. Using the directrix function (generalised to multiparton situations) it is possible to introduce a value $\lambda(\sigma)$ that varies from e.g. $\lambda(\sigma = 0) = 0$ to $\lambda(\sigma = E/\kappa) = \lambda$ (for the variable σ see Eq. (15.10), just as the cms-rapidity y varies from $(-1/2)\Delta y$ to $(+1/2)\Delta y$.

https://doi.org/10.1017/9781009401296.015 Published online by Cambridge University Press